Role of neutron transfer in the sub-barrier fusion cross section in $^{18}O + ^{116}Sn$

Nabendu Kumar Deb,[1] Kushal Kalita,[1,*] Harun Al Rashid,[1] S. Nath,[2] J. Gehlot,[2] N. Madhavan,[2] Rohan Biswas,[2] Rudra N. Sahoo,[3] Pankaj K. Giri,[4] Amar Das,[1] Tapan Rajbongshi,[1] Anamika Parihari,[2] Niraj K. Rai,[5] Saumyajit Biswas,[6] Khushboo,[7] Amritraj Mahato,[4] B. J. Roy,[8,9] A. Vinayak,[10] and Anjali Rani[7]

[1]*Department of Physics, Gauhati University, Guwahati 781014, Assam, India*
[2]*Nuclear Physics Group, Inter-University Accelerator Centre, Aruna Asaf Ali Marg, New Delhi 110067, India*
[3]*Department of Physics, Indian Institute of Technology Ropar, Rupnagar 140001, Punjab, India*
[4]*Department of Physics, Central University of Jharkhand, Ranchi 835205, Jharkhand, India*
[5]*Department of Physics, Banaras Hindu University, Varanasi 221005, Uttar Pradesh, India*
[6]*Department of Physics, Siksha Bhavana, Visva-Bharati, Santiniketan 731235, West Bengal, India*
[7]*Department of Physics and Astrophysics, Delhi University, Delhi 110007, India*
[8]*Nuclear Physics Division, Bhabha Atomic Research Centre, Mumbai 400085, Maharashtra, India*
[9]*Homi Bhabha National Institute, Anushaktinagar, Mumbai 400094, Maharashtra, India*
[10]*Department of Studies in Physics, Karnatak University, Dharwad 580003, Karnataka, India*

(Received 29 October 2019; revised 3 June 2020; accepted 8 July 2020; published 3 September 2020)

Background: In heavy-ion-induced fusion reactions, cross sections in the sub-barrier region are enhanced compared to predictions of the one-dimensional barrier penetration model. This enhancement is often understood by invoking deformation and coupling of the relative motion with low-lying inelastic states of the reaction partners. However, effects of nucleon transfer on fusion below the barrier, especially for the systems having positive Q value neutron transfer (PQNT) channels, are yet to be disentangled completely.
Purpose: We intend to study the role of the PQNT effect on the sub-barrier fusion of the $^{18}O + ^{116}Sn$ system having positive Q value for the two-neutron stripping channel. Also we reflect on the interplay of couplings involved in the system around the Coulomb barrier.
Method: The fusion excitation function was measured at energies from 11% below to 46% above the Coulomb barrier for $^{18}O + ^{116}Sn$ using a recoil mass spectrometer, viz., the Heavy-Ion Reaction Analyser (HIRA). Fusion barrier distributions were extracted from the data. Results from the experiment were analyzed within the framework of the coupled-channels model.
Results: Fusion cross sections at energies below the Coulomb barrier showed strong enhancement compared to predictions of the one-dimensional barrier penetration model. The fusion process is influenced by couplings to the collective excitations with coupling to single- and two-phonon vibrational states of the target and the projectile respectively. Inclusion of the two-neutron transfer channel in the calculation along with these couplings could reproduce the data satisfactorily.
Conclusions: The significant role of PQNT in enhancing the sub-barrier fusion cross section for the chosen system is not observed. It simply reduced the sub-barrier fusion cross section. Therefore, a consistent link between PQNT and sub-barrier fusion enhancement could not be established vividly while comparing the fusion excitation function from this work with the same from other $^{16,18}O$-induced reactions. This clearly points to the need for more experimental as well as theoretical investigation in this field.

DOI: 10.1103/PhysRevC.102.034603

I. INTRODUCTION

Intense research has been going on for the last few decades to understand the interplay between nuclear reaction dynamics and nuclear structure around the barrier [1–5]. Contrary to classical belief, in which fusion between two colliding nuclei takes place only if the incident projectile energy in the center-of-mass (c.m.) frame of reference ($E_{c.m.}$) is more than the Coulomb barrier (V_b), fusion has been found to take place even for $E_{c.m.} \leqslant V_b$. This phenomenon, modeled as the one-dimensional barrier penetration model (1D-BPM), is due to quantum tunnelling of the projectile through the barrier [1,6]. Moreover, for many systems, significant enhancement of fusion cross sections has been observed beyond the 1D-BPM predictions, near and below the Coulomb barrier [7,8].

Such enhancements in sub-barrier fusion cross sections have been attributed to coupling of the relative motion with internal degrees of freedom such as neck formation [9,10], deformation [11–13], zero point motion [14], nuclear shape vibrations [15–20], or nucleon transfer [21–25]. These couplings often lessen the barrier height by modifying the one-

*ku_kalita@yahoo.com

dimensional Coulomb barrier into multiple potential barriers which then cause enhancement of fusion cross sections [26–29]. With the theoretical models available, these effects of inelastic excitations could be explained reasonably well [30–33]. However, the role of neutron transfer in heavy-ion sub-barrier fusion is still not fully resolved. This is mainly because of the challenges of accounting for the intricate mechanism of transfer channels in the theoretical models, because the chargeless neutron, unaffected by the Coulomb barrier, can freely flow from one collision partner to the other even at large internuclear distances [34].

Because of nonexistence of the fusion barrier, neutron transfer ought to be more important than proton transfer to study the effects of transfer channels on fusion. Beckerman *et al.* [35] pioneered in discovering the fact that fusion enhancement near the fusion barrier of ^{58,64}Ni + ^{58,64}Ni, observed experimentally, could be due to possible neutron transfer with positive Q value. Such enhancement due to the appropriate Q value transfer channels was further confirmed by Broglia *et al.* [36] and Zagrebaev [22]. The gain in the kinematic energy of the intermediate states due to such positive Q value neutron transfers (PQNT) is considered an important factor for fusion [37,38]. Based on this idea Stelson *et al.* [39] and Henning *et al.* [40] pointed out that the neutron transfer takes place beyond the barrier distance, thereby promoting the neck formation which provides enough force to overcome the Coulomb barrier.

Following this revelation, a series of studies were done to extricate the PQNT effect on the fusion cross section. It has been observed that large enhancement of the fusion cross section below the uncoupled Coulomb barrier occurred due to neutron transfer channels for the fusing systems having positive Q value for the transfer channel. Systems having PQNT channels such as ^{28}Si + ^{94}Zr [25], ^{40}Ca + ^{70}Zn [41], ^{32}S + ^{48}Ca [42], ^{32}Si + ^{96}Zr, ^{100}Mo, ^{110}Pd [18,43,44], and ^{40}Ca + ^{48}Ca, ^{96}Zr, ^{124,132}Sn [45–50] showed fusion enhancement. Nevertheless, for the system ^{40}Ca + ^{96}Zr, the enhancement could be explained well considering coupling of intrinsic degrees of freedom of ^{96}Zr nuclei [51]. In contrast, there are some systems having PQNT channels, such as ^{18}O + ^{92}Mo, ^{118}Sn [52,53], ^{36}S + ^{58}Ni [54], ^{58}Ni + ^{100}Mo, ^{124}Sn [54–57], ^{60}Ni + ^{100}Mo [58], and ^{132}Sn + ^{58}Ni [59], which do not show any enhancement of the sub-barrier fusion cross sections. Sargsyan *et al.* [60] claimed that sub-barrier fusion enhancement due to neutron transfer with a positive Q value needs to be revisited as the neutron transfer takes place due to the change in nuclear deformation.

Thus the role of PQNT on heavy-ion sub-barrier fusion is ambiguous and inconsistent. More experiments on the systems having one-neutron ($1n$) and two-neutron ($2n$) transfers with positive Q values, as the simplest cases, are required for the consistent development of the hypothesis and, therefore, the improvement of existing theoretical models [61]. Working in this context, we chose ^{18}O + ^{116}Sn system to measure the fusion excitation function and find the probable role of PQNT in the sub-barrier fusion cross section, as emphasized by Zhang *et al.* [62]. We carried out measurements at projectile energies, in the laboratory frame of reference ($E_{\rm lab}$), of 52–86 MeV, i.e., from ≈11% below to ≈46% above the Coulomb barrier. This measurement was understood by performing coupled-channels calculation using the code CCFULL [30]. In this system, the Q value is positive for the $2n$ stripping channel. Results of the current system were compared with the same from ^{16}O + ^{116}Sn [19], which possesses negative Q value for both the $1n$ and $2n$ transfer channels. This is mainly due to the spherical nature of ^{16}O for which the energy of the first 2^+ state is 7 MeV, in contrast to only 2 MeV for the corresponding state of ^{18}O having two neutrons outside the ^{16}O core.

This paper describes the experimental details in Sec. II. Data analysis and results are presented in Sec. III. Sec. IV includes a summary of work done and conclusions.

II. EXPERIMENTAL DETAILS

The experiment was carried out using the Heavy Ion Reaction Analyser (HIRA) [63] at the 15UD Pelletron accelerator facility of the Inter-University Accelerator Centre (IUAC) [64]. The HIRA is a recoil mass spectrometer having Q1-Q2-ED1-M-MD-ED2-Q3-Q4 configuration, where Q, ED, M, and MD stand for quadrupole magnet, electrostatic dipole, magnetic multipole and magnetic dipole, respectively. The HIRA rejects the primary beam background and transports the reaction products to its focal plane.

In the present experiment, having a methodology similar to that of Refs. [11,65], a pulsed ^{18}O beam with 4 μs pulse separation bombarded an isotropically (99.6%) enriched ^{116}Sn target of thickness ≈150 μg/cm^2, prepared on ≈30 μg/cm^2 thick $^{\rm nat}$C backing [66], inside the HIRA target chamber. The targets were mounted with carbon facing the beam. Measurements were done at $E_{\rm lab}$ ranging 52–86 MeV in steps of 1 MeV below the barrier and 2–2.5 MeV above the barrier, covering the energy range $0.89V_{\rm b}$–$1.47V_{\rm b}$. To monitor the beam and for absolute normalization of evaporation residue (ER) cross sections, two solid state silicon detectors were mounted at $\theta_{\rm lab} = \pm 15.5^\circ$ in the horizontal plane. $A \approx 30$ μg/cm^2 thick $^{\rm nat}$C foil was kept 10 cm downstream of the target for reequilibration of the charge state of ERs.

A position-sensitive multiwire proportional counter (MWPC), with an active area of 150 × 50 mm^2 was mounted at the HIRA focal plane for detection of ERs. Time of flight (mTOF) of ERs over the distance from the target to the detector was measured, which helped in distinguishing the ERs from scattered beamlike particles, as shown in Fig. 1 at $E_{\rm c.m.} = 74.3$, 49.9, and 44.6 MeV. The background spectrum shown in the figure was obtained by taking a run of 1 hour with a blank target frame in which no event had been recorded within the ER gate. Such good separation of ERs helped in measuring fusion cross section ($\sigma_{\rm fus}$) down to $E_{\rm lab} = 52$ MeV. List mode data were collected and analyzed offline using the program CANDLE [67].

III. DATA ANALYSIS AND RESULTS

For the present system, ^{18}O + ^{116}Sn, the fusion yield is taken to be equal to the sum of the ER yields because, within the energy range under consideration, the contribution from fission is found to be insignificant [68]. The fusion cross

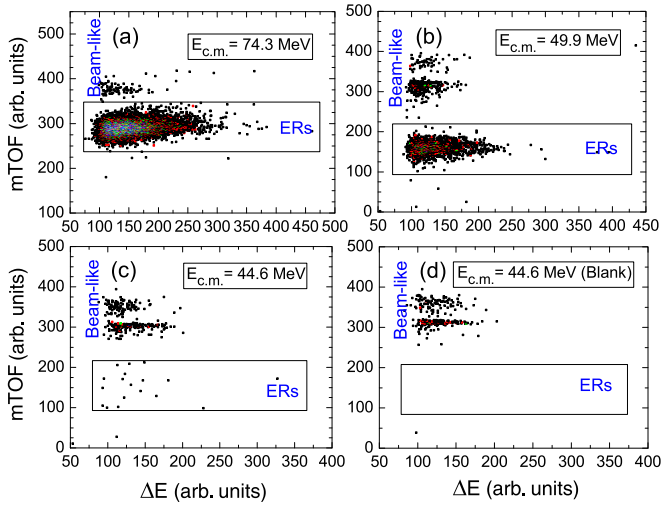

FIG. 1. Two-dimensional scatter plots between ΔE and mTOF obtained for the ^{18}O + ^{116}Sn system at various energies: (a) $E_{\mathrm{c.m.}}$ = 74.3 MeV ($\frac{E_{\mathrm{c.m.}}}{V_{\mathrm{b}}} \approx 1.46$), (b) $E_{\mathrm{c.m.}}$ = 49.9 MeV ($\frac{E_{\mathrm{c.m.}}}{V_{\mathrm{b}}} \approx 0.99$), (c) $E_{\mathrm{c.m.}}$ = 44.6 MeV ($\frac{E_{\mathrm{c.m.}}}{V_{\mathrm{b}}} \approx 0.89$) and (d) same plot at $E_{\mathrm{c.m.}}$ = 44.6 MeV with the blank target. ERs, enclosed within rectangular gate (indicating fusion events), and the beamlike particles are well separated from each other. Here $E_{\mathrm{c.m.}}$ and V_{b} are the energy and the Coulomb barrier in the center-of-mass frame respectively.

section was estimated using the expression

$$\sigma_{\mathrm{fus}} \simeq \sigma_{\mathrm{ER}} = \frac{1}{\varepsilon}\left(\frac{Y_{\mathrm{ER}}}{Y_{\mathrm{M}}}\right)\left(\frac{d\sigma}{d\Omega}\right)_{\mathrm{R}} \Omega_{\mathrm{M}} \qquad (1)$$

where ε is the average transmission efficiency of ERs through the HIRA, Y_{ER} is the ER yield at the HIRA focal plane, Y_{M} is the geometric mean of yields in the two monitor detectors, $(\frac{d\sigma}{d\Omega})_R$ is the Rutherford differential scattering cross section in the laboratory frame of reference, and Ω_{M} is the solid angle subtended by the monitor detectors.

ε is defined as the ratio of the number of ERs reaching the focal plane to the total number of ERs emanating from the target. It is a complex function of various instrument-specific and reaction-specific parameters [69]. Measuring ε for each exit channel at different E_{lab} is very tedious. In the present case, ε was calculated using the semimicroscopic Monte Carlo simulation code TERS [70] following the prescription provided in Ref. [69]. Relative population of different ER exit channels was calculated by the statistical Monte Carlo code PACE4 [68]. The uncertainty in calculating ε is expected to be within 10% [69,71].

The Rutherford differential scattering cross section at each E_{lab} was calculated using the following expression:

$$\left(\frac{d\sigma}{d\Omega}\right)_{\mathrm{R}} = 1.296\left(\frac{Z_{\mathrm{P}}Z_{\mathrm{T}}}{E_{\mathrm{lab}}}\right)^2 \left\{\frac{1}{\sin^4\left(\frac{\theta_{\mathrm{lab}}}{2}\right)} - 2\left[\frac{M_{\mathrm{P}}}{M_{\mathrm{T}}}\right]^2\right\} \qquad (2)$$

where Z_{P}, M_{P}, Z_{T}, and M_{T} denote the atomic number and the mass number of the projectile and the target, respectively.

Thus, using Eq. (1), σ_{fus} were obtained and are tabulated in Table I. Uncertainties in σ_{fus} include the statistical errors and the uncertainty in estimating ε. Figure 2 shows the experimental fusion excitation function for ^{18}O + ^{116}Sn along with the 1D-BPM calculation. Enhancement of σ_{fus} in the sub-barrier region is clearly visible. To understand the reason, the following analysis techniques were adopted.

TABLE I. Fusion cross sections (σ_{fus}) measured experimentally for the ^{18}O + ^{116}Sn system at energies in the center-of-mass frame ($E_{\mathrm{c.m.}}$) and the corresponding errors in cross sections ($\delta\sigma$).

$E_{\mathrm{c.m.}}$ (MeV)	σ_{fus} (mb)	$\pm\delta\sigma$ (mb)
44.6	0.221	0.080
45.5	0.448	0.109
46.4	1.86	0.38
47.3	6.54	0.99
48.1	17.5	2.33
49.0	33.3	4.20
49.9	63.8	8.15
50.8	98.2	12.1
51.6	144.3	17.8
52.7	201.1	24.5
54.2	273.7	33.2
55.9	371.1	50.9
56.8	428.3	50.3
59.0	564.9	64.2
61.2	693.5	81.6
63.3	830.9	100.8
65.5	925.6	107.7
67.7	1025.3	126.3
69.8	1114.0	139.0
72.0	1166.6	147.4
74.3	1271.2	161.0

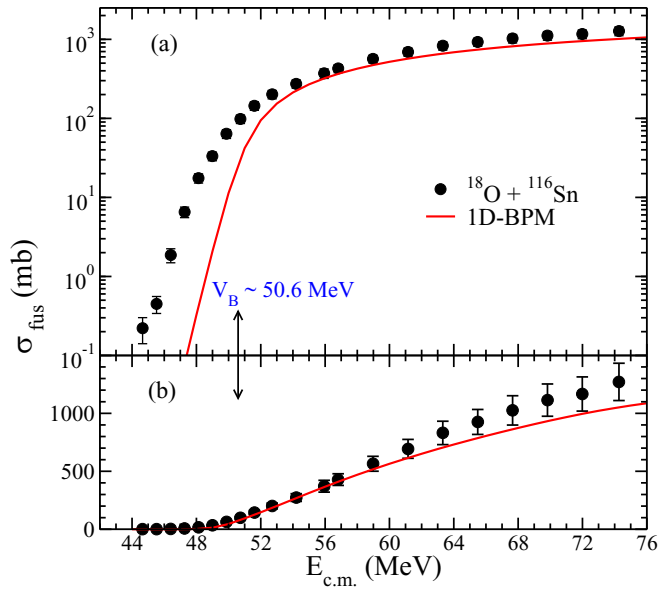

FIG. 2. (a) Experimentally measured fusion excitation function for the ^{18}O + ^{116}Sn system along with the 1D-BPM calculations using CCFULL code. The lower plot (b) shows fusion cross sections in linear scale for better view of the above-barrier energies. Uncertainties of a few data points are smaller than symbol size.

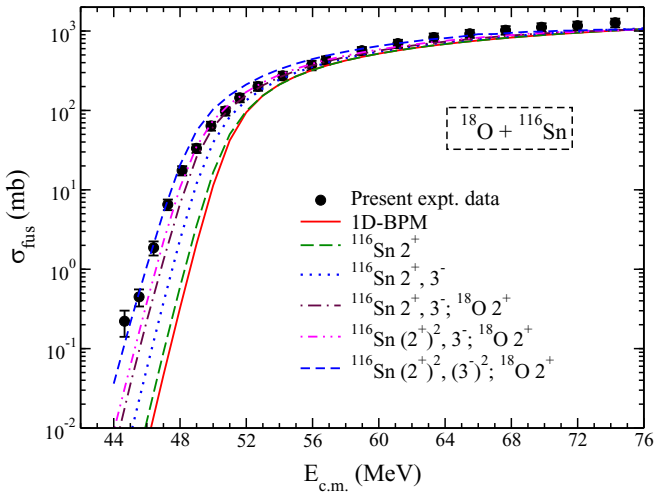

FIG. 3. The experimentally measured excitation function is compared with the 1D-BPM and the different modes of coupling between interacting partners using CCFULL. Fusion cross sections with the inelastic couplings between projectile and target are shown by different curves.

A. Coupled-channels calculation

The code CCFULL calculates σ_{fus} with or without considering inelastic excitations of interacting nuclei. To obtain the 1D-BPM cross sections, calculations were done without including inelastic excitations. In this calculation, Woods-Saxon parametrization of the ion-ion potential [72] was used with values of the depth (V_0), the radius (r_0) and the diffuseness (a_0) parameters of 100 MeV, 1.06 fm, and 0.82 fm, respectively. The values were chosen so as to fit the above-barrier data and produce equivalent Coulomb barrier parameters obtained using Woods-Saxon parametrization of the Akyüz-Winther (AW) potential [73], which are barrier height $V_b = 50.62$ MeV and barrier radius $r_b = 10.45$ fm. The 1D-BPM clearly underpredicts the experimental σ_{fus}.

For further analysis, coupled-channels calculations were done including various low-lying inelastic excitations and transfer channels as shown in Figs. 3 and 4. Table II provides the spectroscopic properties of the interacting nuclei, used in the coupled-channels calculations. The fusion process can be influenced by these parameters. The deformation parameters connected with the transition of multipolarity λ were calculated using the reduced transition probabilities $B(E_\lambda)$ [74,75].

Coupled-channels calculations were done with both ^{18}O and ^{116}Sn as vibrators. To begin with, target excitation with 2^+ vibrational states of ^{116}Sn was considered. Although calculated σ_{fus} was enhanced a bit, compared to that of 1D-BPM, it still underestimated experimental σ_{fus}. 3^- states of ^{116}Sn was then included, which resulted in further enhancement of σ_{fus}, indicating that 3^- state is stronger in this case. Likewise, couplings with other states were included one after another in the CCFULL calculations, as shown in Figs. 3 and 4. Projectile excitations were also added eventually in the calculations. Inclusion of mutual coupling of two-phonon vibrational states including 2^+, 3^-, $2^+ \otimes 3^-$, $(3^-)^2$, $2^+ \otimes (3^-)^2$ of ^{116}Sn (following the prescriptions provided in Ref. [19]) and single-phonon 2^+ vibrational state of ^{18}O in the calculation resulted in overprediction of the experimental σ_{fus} near as well as below the barrier, as shown in Fig. 3. No such combination could reproduce the data in all energy regimes. However, when the two-phonon excitations of the 2^+ vibrational state of ^{18}O—a low-lying state with a high degree of collectivity—is invoked by coupling it mutually with the single-phonon coupling of 2^+ and 3^- states of ^{116}Sn, the result seems to reproduce the experimental data fairly well in the whole energy range. The result obtained by this coupling scheme, shown in Fig. 4, almost overlaps with that of the cross section obtained by mutual coupling of single-phonon 2^+ vibrational state of ^{18}O with the two-phonon 3^- states and single-phonon 2^+ states of ^{116}Sn.

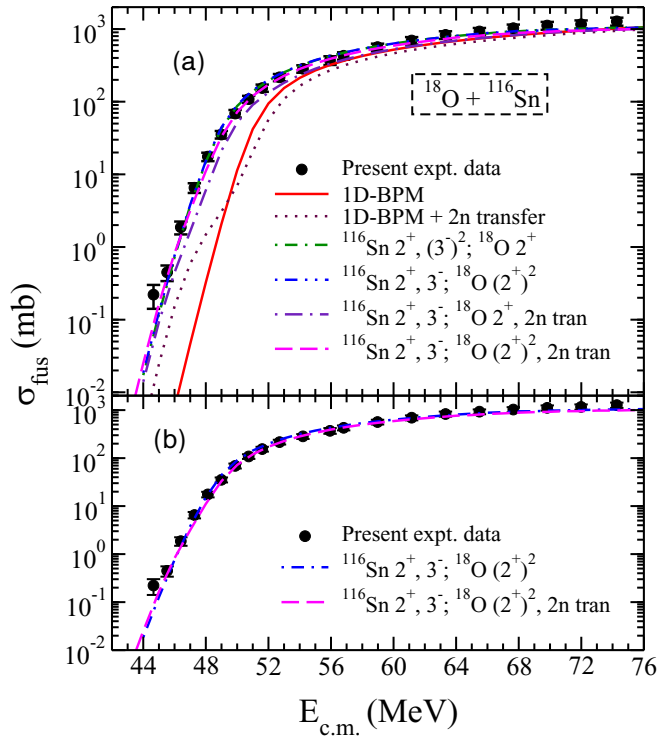

FIG. 4. (a) The experimentally measured excitation function is compared with the coupling of the 2*n* transfer channel beside the inelastic excitations and with different modes of coupling between interacting partners using CCFULL. They are shown by different curves. Panel (b) displays the 2*n* transfer closest fit for a clear view.

TABLE II. Excited states (λ^π) along with their excitation energies (E_λ) and the corresponding deformation parameters (β_λ) for ^{18}O and ^{116}Sn nuclei used in the coupled-channels calculation [19,62].

Nucleus	λ^π	E_λ (MeV)	β_λ
^{18}O	2^+	1.982	0.355
	3^-	5.098	0.39
^{116}Sn	2^+	1.293	0.143
	3^-	2.266	0.213

TABLE III. The Q values for the neutron transfer of the various comparable systems (in MeV). "Q_-" refers to the neutron transfer from the ground states of projectile nuclei to the ground states of target nuclei and the inverse is denoted by "Q_+".

Reactions	Q_{-4n}	Q_{-3n}	Q_{-2n}	Q_{-1n}	Q_{+1n}	Q_{+2n}	Q_{+3n}	Q_{+4n}
^{18}O + ^{116}Sn	−9.218	−5.099	4.081	−1.102	−5.608	−5.548	−12.042	−12.936
^{16}O + ^{116}Sn	−37.079	−29.313	−12.618	−8.721	−5.42	−4.923	−11.268	−11.403
^{16}O + ^{112}Sn	−33.782	−26.475	−10.843	−7.92	−6.645	−6.768	−14.095	−15.119
^{16}O + ^{112}Cd	−38.515	−30.344	−13.305	−9.125	−5.251	−4.181	−10.141	−9.856
^{18}O + ^{148}Nd	−16.049	−10.104	0.225	−3.007	−3.377	−1.061	−4.821	−3.726
^{18}O + ^{92}Mo	−6.804	−2.736	5.559	0.024	−8.715	−11.214	−20.638	−24.187
^{18}O + ^{74}Ge	−10.351	−5.848	3.745	−1.54	−6.241	−5.416	−12.361	−12.927

Transfer channels were included in the coupling scheme next to see the PQNT effect. The present system has a positive Q value of 4.081 MeV for the $2n$ stripping channel. All the other transfer channels have negative Q values, as charted in Table III. The CCFULL code includes the option to couple just one pair of neutron transfer channels between the ground states of the colliding nuclei. Therefore, the code includes only one transfer channel and does not calculate $+2n$, $-2n$, $+1n$, and $-1n$ separately. Initially calculations were done with the $2n$ transfer channel excluding all the inelastic excitations. The resulting cross sections underpredicted the experimental $\sigma_{\rm fus}$ to a large extent. Hence, keeping in mind the claim of Sargsyan *et al.* [60], the calculation was done including both the $2n$ transfer channel and the inelastic excitations. The result is illustrated in Fig. 4, showing fair reproduction of the data when the $2n$ transfer channel is coupled with inelastic excitations of single-phonon and double-phonon vibrational states of the target and projectile respectively, but still underpredicts the inelastic excitations of the same collective states very slightly. The code CCFULL accounts for the transfer channel through the macroscopic transfer coupling form factor, $F_{tr}(r)$. For its estimation, in principle, the transfer cross section and hence the transfer probability measurements are needed [25,76,77], but, since the transfer cross sections have not been measured for the present system, the coupled channel calculations are done with various form factors. Furthermore, even with the experimental data, it is still very difficult to deduce the $F_{tr}(r)$, because the mechanism of transfer coupling is yet unclear in theory. Transfer coupling form factors, which are consistent with the transfer cross sections, are a good practical way to determine the strength of the transfer coupling so that sub-barrier fusion reaction can be reproduced. Such strength is a phenomenological parameter and it is not easy to assign a physical meaning. Therefore, this strength parameter in the form factor is phenomenologically adjusted for the transfer couplings, rather than computing them microscopically. An assumption of such an approach is that all the strength in a Q value distribution for a transfer reaction is concentrated in a single state with a definite value of Q. This indicates the importance of Q value neutron transfer channels in the enhancement of sub-barrier fusion cross section. The coupling potential for the transfer channel is taken to be [30,77]

$$F_{\rm tr}(r) = F\frac{dV_N}{dr}, \tag{3}$$

where V_N is the nuclear interaction potential. For the present system, the neutron transfer coupling has been included in the CCFULL code through transfer coupling strength parameter (F) for two-neutron transfer which is varied in the range from 0.2 to 0.5 fm to obtain an appropriate fit to the experimental fusion cross section. With $F = 0.3$ fm, the CCFULL result gives the best fit to the data. The effect of neutron transfer, here, appears to be a small reduction of the fusion cross section at most energies. The magnitude of this reduction is shown in Fig. 5 which shows the $2n$-transfer and total reaction cross sections as a function of energy. Inelastic excitations which reproduced the data (as shown in Fig. 4) and the inclusion of $2n$ transfer with same collective excitations are shown in Fig. 5. The difference of the fusion cross section is then obtained where we can observe the magnitude of the $2n$ transfer stealing cross section from the fusion channel (shown as the inset in Fig. 5). Hence, the role played by PQNT due to the $2n$ transfer channel in the ^{18}O + ^{116}Sn system appears to be quite significant.

Nucleons transfer between the interacting nuclei in heavy-ion-induced reactions is highly regulated by optimum Q value ($Q_{\rm opt}$). It is seen that all the transfer channels (including neutron stripping), except neutron pickup and proton stripping, are hindered depending on the value of $Q_{\rm opt}$ [78]. In between these two transfer processes, the neutron pickup is more

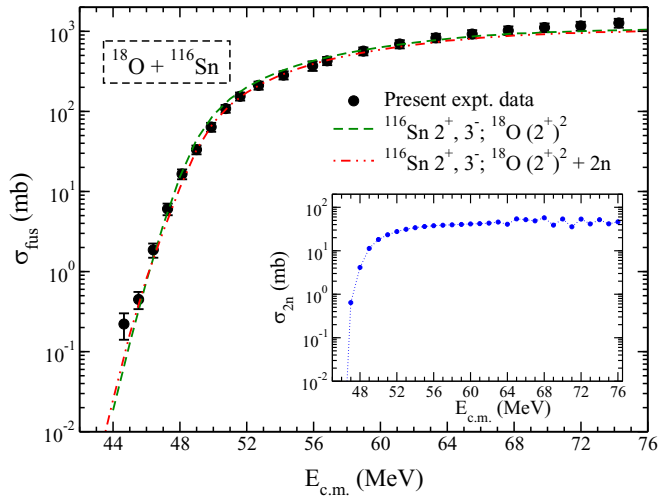

FIG. 5. $2n$ transfer (inset) reducing cross section from the fusion channel from the inelastic curve of the same collective excitation (refer text for details).

probable due to its insensitivity towards the Coulomb barrier. For $Q > 0$ it is a good approximation to take $Q = Q_{\rm opt}$, while for $Q < 0$ it would be at $Q = Q_{gg}$. Practically, the transfer takes place mainly to the excited states, rather than to the ground state [79], and the coupling to the ground state is much weaker [22]. But, in fact, the projectile and target charge, for neutron transfer channels, remains the same, corresponding to which $Q_{\rm opt} = 0$ [80]. Hence, for the interpretation of the present work, the ground state Q value (Q_{gg}) is taken into consideration.

B. Fusion functions

To explore the PQNT effect on fusion reactions further, the fusion function proposed by Prasad *et al.* [81] is applied here for the present system along with the systems ^{16}O + ^{112,116}Sn [19]. The fusion function completely eliminates the influence of optical potential and bound channel coupling effects on $\sigma_{\rm fus}$. It thus helps us make definite conclusions about the effect of deformation of the colliding nuclei and the role played by neutron transfer channels in the fusion process. In this procedure, 1D-BPM does not depend on the system and hence is considered the reference for all the systems [81]. For this, dimensionless variables $E_{\rm red}$ and $\sigma_{\rm red}$ are defined as

$$\sigma_{\rm red} = \frac{2E_{\rm c.m.}\sigma_{\rm fus}}{\hbar\omega R_{\rm b}^2} \tag{4}$$

and

$$E_{\rm red} = \frac{E_{\rm c.m.} - V_{\rm b}}{\hbar\omega} \tag{5}$$

where $\hbar\omega$, $R_{\rm b}$, and $V_{\rm b}$ correspond to the barrier curvature, the barrier radius, and the barrier height, respectively. The variable $E_{\rm red}$ is known as the reduced energy. The barrier parameters are obtained using AW potential parameters in CCFULL calculations. $\sigma_{\rm fus}$ and $E_{\rm c.m.}$ are directly imported from the experimental data. But for 1D-BPM, $\sigma_{\rm fus}$ is obtained in the desired energy ($E_{\rm c.m.}$) range using Wong's expression [82]:

$$\sigma_{\rm fus} = \frac{R_{\rm b}^2\hbar\omega}{2E_{\rm c.m.}} \ln\left[1 + \exp\left(2\pi\frac{E_{\rm c.m.} - V_{\rm b}}{\hbar\omega}\right)\right]. \tag{6}$$

Figure 6 shows the plot of $\sigma_{\rm red}$ versus $E_{\rm red}$ for the three systems in which only the present system has positive Q value for the $2n$ transfer channel, as shown in Table III and in the inset of Fig. 6. In the figure, $\sigma_{\rm red}$ of the present system ^{18}O + ^{116}Sn deviates strongly from that of ^{16}O + ^{112,116}Sn below the Coulomb barrier. This can be attributed to the PQNT effect. Moreover, after neutron transfer, ^{18}O ($\beta_2 = 0.355$) + ^{116}Sn ($\beta_2 = 0.1$) → ^{16}O ($\beta_2 = 0.36$) + ^{118}Sn ($\beta_2 = 0.1$); there is an increment in the deformation of the interacting nuclei, lowering the barrier height and thus increasing $\sigma_{\rm fus}$.

C. Fusion barrier distribution

The fusion barrier distributions (BDs) are highly sensitive to higher order deformation of nuclei. To analyze the nature of couplings involved in the sub-barrier fusion, the fusion BD is employed. The experimental BDs were obtained from measured $\sigma_{\rm fus}$ by double differentiation of energy times the corresponding $\sigma_{\rm fus}$ with respect to the energy [1,27], using the

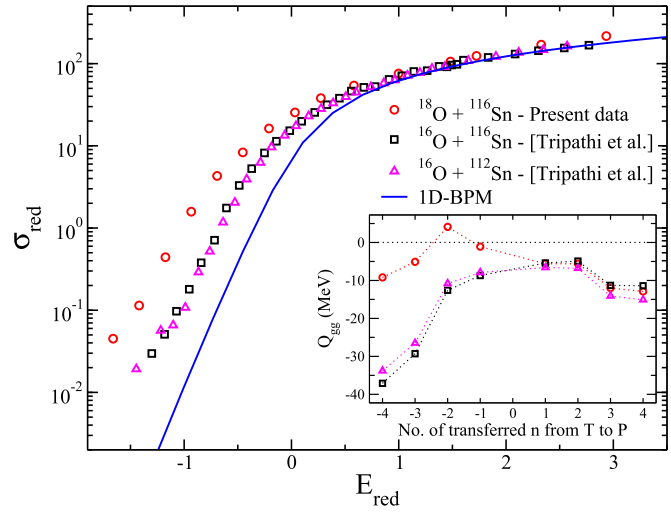

FIG. 6. Comparison of fusion excitation function for similar systems (from Tripathi *et al.* [19]) with the present one in terms of reduced fusion function (refer to text for details). The inset shows the ground state Q values (Q_{gg}) for the systems considered for comparison here (see Table III).

three-point difference formula [83], i.e., at energy $(E_1 + 2E_2 + E_3)/4$:

$$D_{\rm fus}(E) = \frac{d^2(E\sigma_{\rm fus})}{dE^2} = \left[\frac{(E\sigma_{\rm fus})_3 - (E\sigma_{\rm fus})_2}{E_3 - E_2} - \frac{(E\sigma_{\rm fus})_2 - (E\sigma_{\rm fus})_1}{E_2 - E_1}\right] \times \frac{2}{E_3 - E_1}, \tag{7}$$

where $(E\sigma_{\rm fus})_{\rm i}$ corresponds to $E_{\rm i}$. The statistical error, δ, associated with $D_{\rm fus}(E)$ at energy E was calculated as

$$\delta = \left(\frac{E}{\Delta E^2}\right)\left[(\delta\sigma_{\rm fus})_1^2 + 4(\delta\sigma_{\rm fus})_2^2 + (\delta\sigma_{\rm fus})_3^2\right]^{\frac{1}{2}}, \tag{8}$$

where $(\delta\sigma_{\rm fus})_i$ are the absolute errors in $(\sigma_{\rm fus})_i$. The error increases with increasing absolute error in $\sigma_{\rm fus}$ and increasing energy. For small error in $\sigma_{\rm fus}$, the second derivation gives large error; thereby poorly defining the experimental BD at higher energies. Thus the low energy regime will be very essential for the BD curve analysis. Figure 7 shows the fusion BD obtained for the ^{18}O + ^{116}Sn system. The experimental BD are broad and have two peaks around the barrier as compared to the 1D-BPM. This could be due to the inelastic coupling of colliding nuclei as described in Fig. 3. We also note that, on considering only the $2n$ transfer channel, the barrier peak shifts slightly towards higher energy than that of the corresponding 1D-BPM, thus not explaining the experimental BD. But when the inelastic coupling effect was considered, the experimental BD was reproduced reasonably well in almost the entire energy regime. The inelastic effect considered is the coupling of the same collective excitations comprising the inelastic couplings of single-phonon and double-phonon vibrational states of target and projectile respectively, which reasonably matched the experimental data in Fig. 4. However,

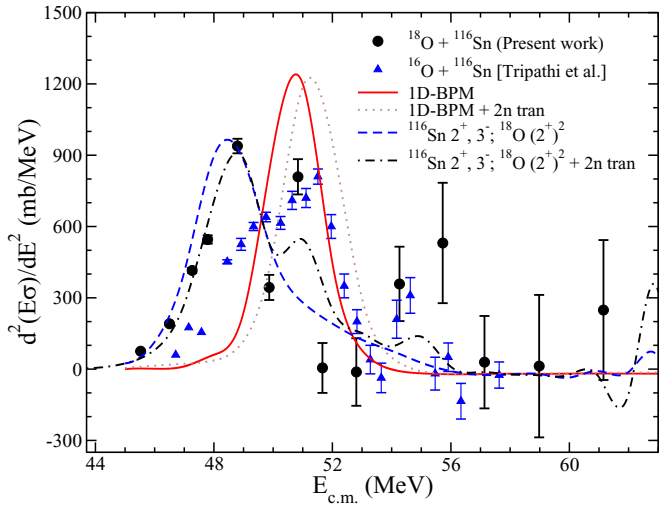

FIG. 7. The fusion barrier distribution for the ^{18}O + ^{116}Sn system extracted from fusion excitation functions are compared with the CCFULL results and with that of the similar system ^{16}O + ^{116}Sn (Tripathi *et al.* [19]). Lines and curves are self-explanatory.

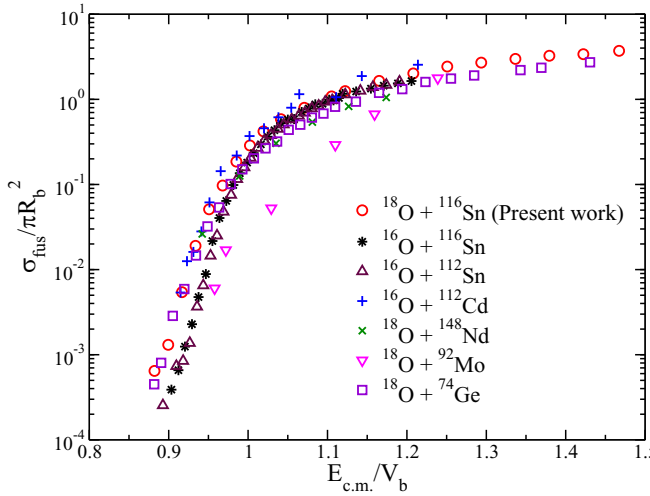

FIG. 8. Comparison of fusion excitation function for the present system with that of the typical systems with ^{16,18}O as projectile on a reduced scale (refer to text for the appropriate references and details).

when the same inelastic couplings of single- and double-phonon vibrational excitation states of the target and projectile respectively along with the 2*n* transfer channel were considered, the barrier peak not only shifted by a slight amount towards higher energy, especially in the low energy regime, but also decreased slightly, as a result of which it matched the experimental barrier peak in a much better way. The major effect of including neutron transfer thus seems to be to shift the peak of the distribution towards slightly higher energies (both for the coupling to the 1D barrier and the coupling to collective excitations). Therefore, the PQNT effect is visible in the present system for interpreting σ_{fus}. The BD of this system is also compared with that of ^{16}O + ^{116}Sn, and the difference is clearly visible as the peak for the present system is towards lower energy and is very broad in the case of ^{16}O + ^{116}Sn, so it is difficult to make any definitive conclusion from this comparison on the attribution of the PQNT effect.

D. Comparison with other similar systems

For further systematic analysis, a comparison was drawn between the systems with ^{16}O and ^{18}O as projectiles in the sub-barrier region on reduced scale, as shown in Fig. 8. The systems considered were ^{16}O + ^{112,116}Sn, ^{16}O + ^{112}Cd and ^{18}O + ^{148}Nd, ^{92}Mo, ^{74}Ge [19,34,52,84,85]. The corresponding *Q* values of these systems are listed in Table III. The scale was reduced to factor out the differences in size and the Coulomb barriers of different systems. Enhancement of σ_{fus} is markedly evident for the present system as well as for ^{18}O + ^{148}Nd which is due to the PQNT effect. But for ^{18}O + ^{74}Ge, the enhancement is completely attributed to inelastic couplings, although the system has positive *Q* value for the 2*n* transfer channel. The PQNT effect does not appear to play any role in this system. The shape of the excitation function of ^{18}O + ^{92}Mo is completely different from the rest of the systems: it does not show any sign of enhancement. The enhancement displayed by ^{16}O + ^{112}Cd is mainly due to the inelastic couplings. The systems ^{16}O + ^{112,116}Sn do not show any such enhancements as these systems have all negative *Q* value transfer channels. Thus the relation between sub-barrier fusion enhancement and the PQNT effect observed in the present system vividly stands out from the rest. However, this comparison does not yield a consistent and unambiguous conclusion about effects of PQNT on sub-barrier fusion enhancement.

IV. SUMMARY AND CONCLUSIONS

In summary, the fusion excitation function was measured for ^{18}O + ^{116}Sn, which has a positive *Q* value for the 2*n* transfer channel. The measurement was done with the HIRA in the energy range of 11% below to 46% above the Coulomb barrier to explore the PQNT effect on sub-barrier fusion. The experimentally measured fusion excitation function was compared with the coupled-channels calculations using the CCFULL model. Experimental σ_{fus} was found to be significantly larger with respect to results from the 1D-BPM calculation. Reasonable fits to the data were obtained by considering various inelastic couplings in the coupled-channels calculation. The fusion process of the present system is influenced by coupling to the collective excitations with coupling to single- and two-phonon states of surface vibrations of target and projectile respectively. The inclusion of the 2*n* transfer channel in the calculation along with the same collective mode of inelastic excitation reproduced the data satisfactorily. While the effect of PQNT somewhat improves the fit to the experimental data, the role of PQNT, in fact, apparently serves to reduce the sub-barrier fusion cross section for the present system. Even the BDs extracted from the data supported this fact. The fusion excitation function was further compared with a few other system having PQNT for the 2*n* stripping channel. The comparison indicated that the link between the PQNT effect and the sub-barrier fusion enhancement is highly

inconsistent. Thus more experimental studies are desired and improvements in coupled-channels models are called for.

ACKNOWLEDGMENTS

The authors are grateful to the Pelletron staff of IUAC for smooth operation of the accelerator during the experiment and the Target Development Laboratory of IUAC for assistance in preparing isotopic targets of requisite thickness. One of the authors (N.K.D.) acknowledges the Council of Scientific and Industrial Research (CSIR), New Delhi for support via a Junior Research Fellowship and Grant No. 09/059(0056)/2014-EMR-I in order to carry out this work.

[1] M. Dasgupta, D. J. Hinde, N. Rowley, and A. M. Stefanini, Annu. Rev. Nucl. Part. Sci. **48**, 401 (1998).
[2] G. Montagnoli and A. M. Stefanini, Eur. Phy. J. A **53**, 169 (2017).
[3] M. Beckerman, Rep. Prog. Phys. **51**, 1047 (1988).
[4] S. G. Steadman and M. J. Rhoades-Brown, Annu. Rev. Nucl. Part. Sci. **36**, 649 (1986).
[5] A. B. Balantekin and N. Takigawa, Rev. Mod. Phys. **70**, 77 (1998).
[6] G. Gamow, Z. Phys. **51**, 204 (1928).
[7] J. D. Bierman, P. Chan, J. F. Liang, M. P. Kelly, A. A. Sonzogni, and R. Vandenbosch, Phys. Rev. Lett. **76**, 1587 (1996).
[8] K. Hagino, N. Takigawa, M. Dasgupta, D. J. Hinde, and J. R. Leigh, Phys. Rev. Lett. **79**, 2014 (1997).
[9] C. E. Aguiar, V. C. Barbosa, L. F. Canto, and R. Donangelo, Nucl. Phys. A **472**, 571 (1987).
[10] C. E. Aguiar, L. F. Canto, and R. Donangelo, Phys. Rev. C **31**, 1969 (1985).
[11] T. Rajbongshi, K. Kalita, S. Nath, J. Gehlot, T. Banerjee, I. Mukul, R. Dubey, N. Madhavan, C. J. Lin, A. Shamlath, P. V. Laveen, M. Shareef, N. Kumar, P. Jisha, and P. Sharma, Phys. Rev. C **93**, 054622 (2016).
[12] J. R. Leigh, M. Dasgupta, D. J. Hinde, J. C. Mein, C. R. Morton, R. C. Lemmon, J. P. Lestone, J. O. Newton, H. Timmers, J. X. Wei, and N. Rowley, Phys. Rev. C **52**, 3151 (1995).
[13] R. G. Stokstad and E. E. Gross, Phys. Rev. C **23**, 281 (1981).
[14] H. Esbensen, Nucl. Phy. A **352**, 147 (1981).
[15] J. O. Newton, C. R. Morton, M. Dasgupta, J. R. Leigh, J. C. Mein, D. J. Hinde, H. Timmers, and K. Hagino, Phys. Rev. C **64**, 064608 (2001).
[16] A. M. Stefanini, G. Fortuna, A. Tivelli, W. Meczynski, S. Beghini, C. Signorini, S. Lunardi, and M. Morando, Phys. Rev. C **30**, 2088 (1984).
[17] C. R. Morton, M. Dasgupta, D. J. Hinde, J. R. Leigh, R. C. Lemmon, J. P. Lestone, J. C. Mein, J. O. Newton, H. Timmers, N. Rowley, and A. T. Kruppa, Phys. Rev. Lett. **72**, 4074 (1994).
[18] A. M. Stefanini, D. Ackermann, L. Corradi, J. H. He, G. Montagnoli, S. Beghini, F. Scarlassara, and G. F. Segato, Phys. Rev. C **52**, R1727(R) (1995).
[19] V. Tripathi, L. T. Baby, J. J. Das, P. Sugathan, N. Madhavan, A. K. Sinha, P. V. Madhusudhana Rao, S. K. Hui, R. Singh, and K. Hagino, Phys. Rev. C **65**, 014614 (2001).
[20] L. T. Baby, V. Tripathi, J. J. Das, P. Sugathan, N. Madhavan, A. K. Sinha, M. C. Radhakrishna, P. V. Madhusudhana Rao, S. K. Hui, and K. Hagino, Phys. Rev. C **62**, 014603 (2000).
[21] V. Y. Denisov, Eur. Phys. J. A **7**, 87 (2000).
[22] V. I. Zagrebaev, Phys. Rev. C **67**, 061601(R) (2003).
[23] S. Kalkal, S. Mandal, N. Madhavan, A. Jhingan, E. Prasad, R. Sandal, S. Nath, J. Gehlot, R. Garg, Gayatri Mohanto, M. Saxena, S. Goyal, S. Verma, B. R. Behera, S. Kumar, U. D. Pramanik, A. K. Sinha, and R. Singh, Phys. Rev. C **83**, 054607 (2011).
[24] L. T. Baby, V. Tripathi, D. O. Kataria, J. J. Das, P. Sugathan, N. Madhavan, A. K. Sinha, M. C. Radhakrishna, N. M. Badiger, N. G. Puttaswamy, A. M. Vinodkumar, and N. V. S. V. Prasad, Phys. Rev. C **56**, 1936 (1997).
[25] S. Kalkal, S. Mandal, N. Madhavan, E. Prasad, S. Verma, A. Jhingan, R. Sandal, S. Nath, J. Gehlot, B. R. Behera, M. Saxena, S. Goyal, D. Siwal, R. Garg, U. D. Pramanik, S. Kumar, T. Varughese, K. S. Golda, S. Muralithar, A. K. Sinha, and R. Singh, Phys. Rev. C **81**, 044610 (2010).
[26] O. A. Capurro, J. E. Testoni, D. Abriola, D. E. DiGregorio, J. O. Fernandez Niello, G. V. Marti, A. J. Pacheco, M. R. Spinella, M. Ramirez, C. Balpardo, and M. Ortega, Phys. Rev. C **65**, 064617 (2002).
[27] N. Rowley, G. R. Satchler, and P. H. Stelson, Phys. Lett. B **254**, 25 (1991).
[28] L. F. Canto, P. R. S. Gomes, R. Donangelo, and M. S. Hussein, Phys. Rep. **424**, 1 (2006).
[29] C. H. Dasso and S. Landowne, Comput. Phys. Commun. **46**, 187 (1987).
[30] K. Hagino, N. Rowley, and T. Kruppa, Comput. Phys. Commun. **123**, 143 (1999).
[31] K. Hagino and N. Takigawa, Prog. Theor. Phys. **128**, 1061 (2012).
[32] V. I. Zagrebaev, A. S. Denikin, A. V. Karpov, A. P. Alekseev, M. A. Naumenko, V. A. Rachkov, V. V. Samarin, and V. V. Saiko, NRV web knowledge base on low-energy nuclear physics, http://nrv.jinr.ru/.
[33] V. I. Zagrebaev, Phys. Rev. C **64**, 034606 (2001).
[34] H. M. Jia, C. J. Lin, F. Yang, X. X. Xu, H. Q. Zhang, Z. H. Liu, L. Yang, S. T. Zhang, P. F. Bao, and L. J. Sun, Phys. Rev. C **86**, 044621 (2012).
[35] M. Beckerman, M. Salomaa, A. Sperduto, H. Enge, J. Ball, A. DiRienzo, S. Gazes, Y. Chen, J. D. Molitoris, and Mao Naifeng, Phys. Rev. Lett. **45**, 1472 (1980).
[36] R. A. Broglia, C. H. Dasso, S. Landowne, and A. Winther, Phys. Rev. C **27**, 2433(R) (1983).
[37] S. Y. Lee, Phys. Rev. C **29**, 1932 (1984).
[38] C. H. Dasso and A. Vitturi, Phys. Rev. C **50**, R12(R) (1994).
[39] P. H. Stelson, H. J. Kim, M. Beckerman, D. Shapira, and R. L. Robinson, Phys. Rev. C **41**, 1584 (1990).
[40] W. Henning, F. L. H. Wolfs, J. P. Schiffer, and K. E. Rehm, Phys. Rev. Lett. **58**, 318 (1987).
[41] Khushboo, N. Madhavan, S. Nath, A. Jhingan, J. Gehlot, B. Behera, S. Verma, S. Kalkal, and S. Mandal, Phys. Rev. C **100**, 064612 (2019).
[42] G. Montagnoli, A. M. Stefanini, H. Esbensen, C. L. Jiang, L. Corradi, S. Courtin, E. Fioretto, A. Goasduff, J. Grebosz, F. Haas, M. Mazzocco, C. Michelagnoli, T. Mijatovic, D.

Montanari, C. Parascandolo, K. E. Rehm, F. Scarlassara, S. Szilner, X. D. Tang, and C. A. Ur, Phys. Rev. C **87**, 014611 (2013).
[43] H. Q. Zhang, C. J. Lin, F. Yang, H. M. Jia, X. X. Xu, Z. D. Wu, F. Jia, S. T. Zhang, Z. H. Liu, A. Richard, and C. Beck, Phys. Rev. C **82**, 054609 (2010).
[44] H.-J. Hennrich, G. Breitbach, W. Kühn, V. Metag, R. Novotny, D. Habs, and D. Schwalm, Phys. Lett. B **258**, 275 (1991).
[45] M. Trotta, A. M. Stefanini, L. Corradi, A. Gadea, F. Scarlassara, S. Beghini, and G. Montagnoli, Phys. Rev. C **65**, 011601(R) (2001).
[46] H. A. Aljuwair, R. J. Ledoux, M. Beckerman, S. B. Gazes, J. Wiggins, E. R. Cosman, R. R. Betts, S. Saini, and O. Hansen, Phys. Rev. C **30**, 1223 (1984).
[47] H. Timmers, D. Ackermann, S. Beghini, L. Corradi, J. H. He, G. Montagnoli, F. Scarlassara, A. M. Stefanini, and N. Rowley, Nucl. Phys. A **633**, 421 (1998).
[48] F. Scarlassara, S. Beghini, G. Montagnoli, G. F. Segato, D. Ackermann, L. Corradi, C. J. Lin, A. M. Stefanini, and L. F. Zheng, Nucl. Phys. A **672**, 99 (2000).
[49] J. J. Kolata, A. Roberts, A. M. Howard, D. Shapira, J. F. Liang, C. J. Gross, R. L. Varner, Z. Kohley, A. N. Villano, H. Amro, W. Loveland, and E. Chavez, Phys. Rev. C **85**, 054603 (2012).
[50] G. Montagnoli, A. M. Stefanini, C. L. Jiang, H. Esbensen, L. Corradi, S. Courtin, E. Fioretto, A. Goasduff, F. Haas, A. F. Kifle, C. Michelagnoli, D. Montanari, T. Mijatovic, K. E. Rehm, R. Silvestri, P. P. Singh, F. Scarlassara, S. Szilner, X. D. Tang, and C. A. Ur, Phys. Rev. C **85**, 024607 (2012).
[51] G. Pollarolo and A. Winther, Phys. Rev. C **62**, 054611 (2000).
[52] M. Benjellom, W. Galster, and J. Vervier, Nucl. Phys. A **560**, 715 (1993).
[53] P. Jacobs, Z. Fraenkel, G. Mamane, and I. Tserruya, Phys. Lett. B **175**, 271 (1986).
[54] A. M. Stefanini, G. Fortuna, R. Pengo, W. Meczynski, G. Montagnoli, L. Corradi, A. Tivelli, S. Beghini, C. Signorini, S. Lunardi, M. Morando, and F. Soramel, Nucl. Phys. A **456**, 509 (1986).
[55] F. Scarlassara, G. Montagnoli, E. Fioretto, C. L. Jiang, A. M. Stefanini, L. Corradi, B. B. Back, N. Patel, K. E. Rehm, D. Sewerinyak, P. P. Singh, X. D. Tang, C. M. Deibel, B. Di Giovine, J. P. Greene, H. D. Henderson, M. Notani, S. T. Marley, and S. Zhu, EPJ Web Conf. **17**, 05002 (2011).
[56] F. L. H. Wolfs, Phys. Rev. C **36**, 1379 (1987).
[57] K. T. Lesko, W. Henning, K. E. Rehm, G. Rosner, J. P. Schiffer, G. S. F. Stephans, B. Zeidman, and W. S. Freeman, Phys. Rev. C **34**, 2155 (1986).
[58] A. M. Stefanini, G. Montagnoli, F. Scarlassara, C. L. Jiang, H. Esbensen, E. Fioretto, L. Corradi, B. B. Back, C. M. Deibel, B. Di Giovine, J. P. Greene, H. D. Henderson, S. T. Marley, M. Notani, N. Patel, K. E. Rehm, D. Sewerinyak, X. D. Tang, C. Ugalde, and S. Zhu, Eur. Phys. J. A **49**, 63 (2013).
[59] Z. Kohley, J. F. Liang, D. Shapira, R. L. Varner, C. J. Gross, J. M. Allmond, A. L. Caraley, E. A. Coello, F. Favela, K. Lagergren, and P. E. Mueller, Phys. Rev. Lett. **107**, 202701 (2011).
[60] V. V. Sargsyan, G. G. Adamian, N. V. Antonenko, W. Scheid, and H. Q. Zhang, Phys. Rev. C **85**, 024616 (2012).
[61] V. A. Rachkov, A. V. Karpov, A. S. Denikin, and V. I. Zagrebaev, Phys. Rev. C **90**, 014614 (2014).
[62] G. L. Zhang, X. X. Liu, and C. J. Lin, Phys. Rev. C **89**, 054602 (2014).
[63] A. K. Sinha, N. Madhavan, J. J. Das, P. Sugathan, D. O. Kataria, A. P. Patro, and G. K. Mehta, Nucl. Instrum. Methods Phys. Res., Sect. A **339**, 543 (1994).
[64] D. Kanjilal, S. Chopra, M. M. Narayanan, I. S. Iyer, V. Jha, R. Joshi, and S. K. Datta, Nucl. Instrum. Methods Phys. Res., Sect. A **328**, 97 (1993).
[65] R. N. Sahoo, M. Kaushik, A. Sood, P. Kumar, A. Sharma, S. Thakur, P. P. Singh, P. K. Raina, Md. M. Shaikh, R. Biswas, A. Yadav, J. Gehlot, S. Nath, N. Madhavan, V. Srivastava, M. K. Sharma, B. P. Singh, R. Prasad, A. Rani, A. Banerjee, U. Gupta, N. K. Deb, and B. J. Roy, Phys. Rev. C **99**, 024607 (2019).
[66] N. K. Deb, K. Kalita, S. R. Abhilash, P. K. Giri, and D. Kabiraj, Proc. DAE Symp. Nucl. Phys. **63**, 1070 (2018).
[67] E. T. Subramaniam, K. Rani, B. P. Ajith Kumar, and R. K. Bhowmik, Rev. Sci. Instr. **77**, 096102 (2006).
[68] A. Gavron, Phys. Rev. C **21**, 230 (1980).
[69] S. Nath, P. V. M. Rao, Santanu Pal, J. Gehlot, E. Prasad, G. Mohanto, S. Kalkal, J. Sadhukhan, P. D. Shidling, K. S. Golda, A. Jhingan, N. Madhavan, S. Muralithar, and A. K. Sinha, Phys. Rev. C **81**, 064601 (2010).
[70] S. Nath, Comput. Phys. Commun. **180**, 2392 (2009).
[71] S. Nath, J. Gehlot, E. Prasad, Jhilam Sadhukhan, P. D. Shidling, N. Madhavan, S. Muralithar, K. S. Golda, A. Jhingan, T. Varughese, P. V. Madhusudhana Rao, A. K. Sinha, and S. Pal, Nucl. Phys. A **850**, 22 (2011).
[72] R. A. Broglia and A. Winther, *Heavy Ion Reaction: Lecture Notes*, Vol. 1: Elastic and Inelastic Reactions (Benjamin/Cummings, Reading, MA, 1981).
[73] Ö. Akyüz and A. Winther, Nuclear structure and heavy-ion reactions, in *Proceedings of the International School of Physics "Enrico Fermi," Course LXXVII, Varenna*, edited by R. A. Broglia *et al.* (North Holland, Amsterdam, 1981).
[74] S. Raman, C. H. Malarkey, W. T. Milner, C. W. Nestor, and P. H. Stelson, At. Data Nucl. Data Tables **36**, 1 (1987).
[75] R. H. Spear, At. Data Nucl. Data Tables **42**, 55 (1989).
[76] S. Saha, Y. K. Agarwal, and C. V. K. Baba, Phys. Rev. C **49**, 2578 (1994).
[77] C. H. Dasso and G. Pollarolo, Phys. Lett. B **155**, 223 (1985); C. H. Dasso and A. Vitturi, *ibid*. **179**, 337 (1986).
[78] L. Corradi, G. Pollarolo, and S. Szilner, J. Phys. G: Nucl. Part. Phys. **36**, 113101 (2009).
[79] L. Corradi, S. Szilner, G. Pollarolo, G. Colò, P. Mason, E. Farnea, E. Fioretto, A. Gadea, F. Haas, D. Jelavić-Malenica, N. Mărginean, C. Michelagnoli, G. Montagnoli, D. Montanari, F. Scarlassara, N. Soić, A. M. Stefanini, C. A. Ur, and J. J. Valiente-Dobón, Phys. Rev. C **84**, 034603 (2011)
[80] W. Henning, Y. Eisen, H.-J. Körner, D. G. Kovar, J. P. Schiffer, S. Vigdor, and B. Zeidman, Phys. Rev. C **17**, 2245(R) (1978)
[81] N. V. S. V. Prasad, A. M. Vinodkumar, A. K. Sinha, K. M. Varier, D. L. Sastry, N. Madhavan, P. Sugathan, D. O. Kataria, and J. J. Das, Nucl. Phys. A **603**, 176 (1996).
[82] C. Y. Wong, Phys. Rev. Lett. **31**, 766 (1973).
[83] N. Rowley, Nucl. Phys. A **538**, 205c (1992).
[84] D. Ackermann, L. Corradi, D. R. Napoli, C. M. Petrache, P. Spolaore, A. M. Stefanini, F. Scarlassara, S. Beghini, G. Montagnoli, G. F. Segato, and C. Signorini, Nucl. Phys. A **575**, 374 (1994).
[85] R. Broda, M. Ishihara, B. Herskind, H. Oeschler, S. Ogaza, and H. Ryde, Nucl. Phys. A **248**, 356 (1975).